Response to comment from Reviewer #1

"1. Why the latitudinal bands of 30-50 are left out? It covers a considerably large area, and may be more subjective to the horizontal mixing than the polar region. Even it may be messy and don't show an as good consistency among forcing agents and across models as the polar regions or the tropical region, it still worth reporting. Furthermore, the 50S-90S may not be a good representation of the Southern Hemisphere extratropics. This is because many models suffer a too strong southern polar vortex and hence the simulated southern polar stratosphere is too isolated. This can be hinted from Fig. 4a and Fig. S4, where a clear barrier is seen near 60S."

We first note that the response of ΔSWV_{slow} to surface temperature as a function of latitude is plotted in Fig. 5a of the submitted manuscript. We also reported the regression slope of ΔSWV_{fast} vs cold point temperature fast response in Fig. 5b of the submitted manuscript.

However, to more clearly answer the reviewer's question, Figure R1 below shows the equilibrium ΔSWV_{slow} and ΔSWV_{fast} and their contribution to the total equilibrium ΔSWV for water vapor averaged at 200 hPa 30°N-50°N and 30°S-50°S. In Figure R2 below, we also show the slope of ΔSWV_{slow} annual mean time series vs surface temperature time series for water vapor averaged at 200 hPa 30°N-50°N and 30°S-50°S. We will include both of these figures in the supplement. The results in the 30-50 degree latitude band show larger magnitudes compared to the results in the 50-90 degree latitude band. However, our major conclusions remain the same: The slow response plays a dominant role and contributes to close to 100% of the total response for most perturbations; The sensitivity shows general agreement across different perturbations.

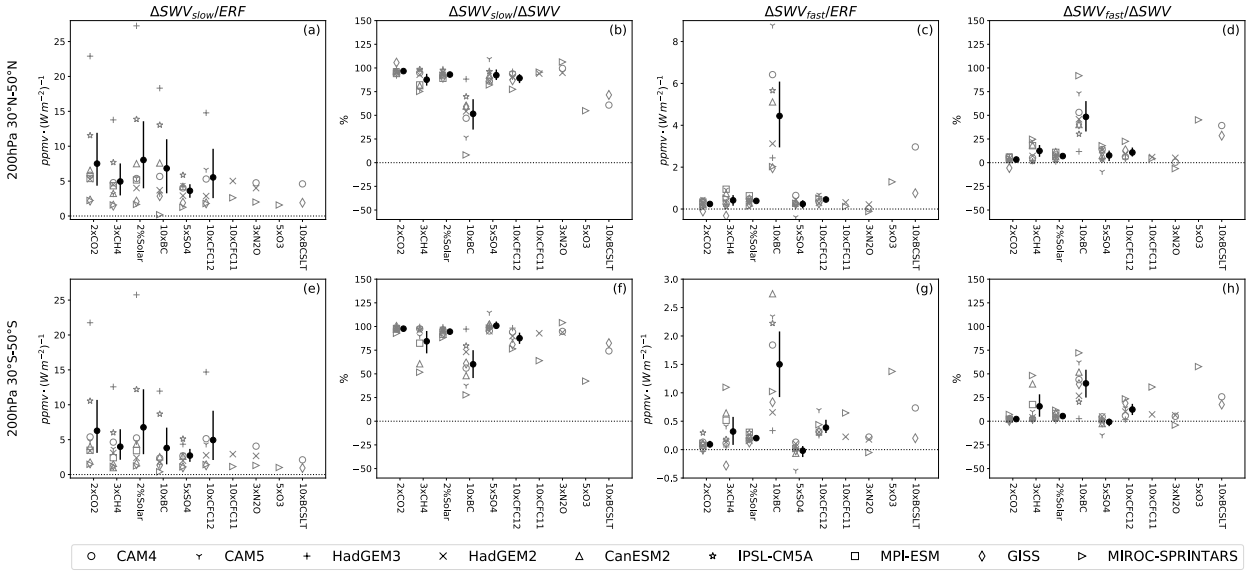

Figure R1: Same as Figure 1 in the submitted paper, but for 200 hPa 30°N-50°N (a-d) and 200 hPa 30°S-50°S (e-h).

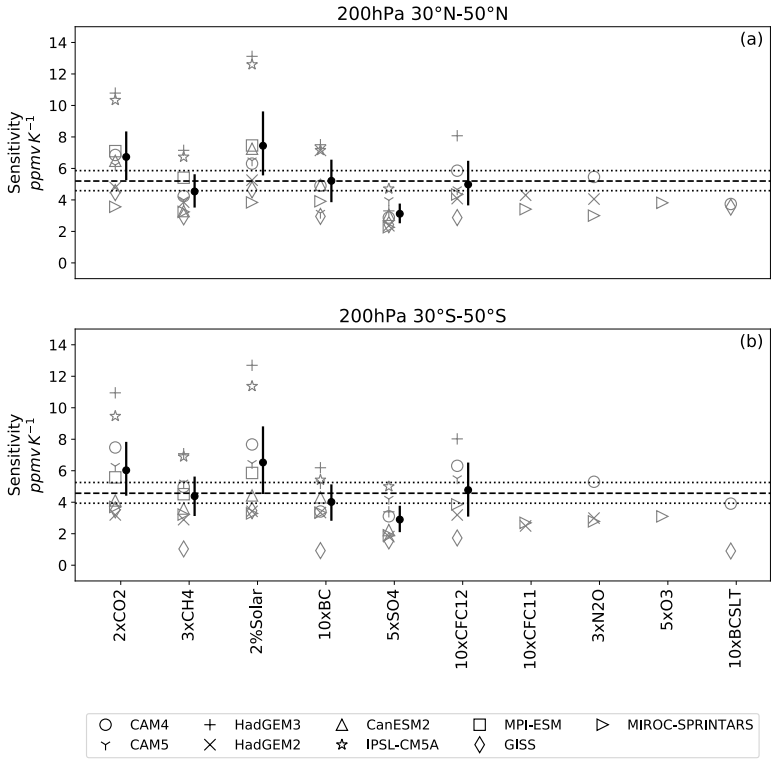

Figure R2: Same as Figure 3, but for 200 hPa 30°N-50°N (a) and 200 hPa 30°S-50°S (b).

"2. The regression method to get the equilibrium water vapor response seems to be unnecessarily complicate, especially the results are not too different from the simple average of the last 30 years. The authors first fit the radiative flux and water vapor time series with an exponential function, then regress the last 30 years of the fitted function. All these fitting and regression have potential introduce artificial biases and uncertainties. Recent studies also show that the ECS from the Gregory method may not be a good estimate of the true ECS (e.g. Winton et al. 2020). In addition, without a sufficiently long simulation, one can not validate whether the "equilibrium" from the regression is the true equilibrium. It makes more sense to me to simply use the average of the last 30 years while acknowledging that the models have not fully reached the equilibrium."

We initially did approximate equilibrium ΔSWV using averages of the last 30 years of the runs. However, we analyzed one model that was run for 2600 years and found that the last 30 years of a 100- or 150-year run significantly underestimated the equilibrium. Thus, we developed the method that we presently use in the paper to better produce equilibrium estimates and validated it in the 2600-year model run, which is close to its equilibrium climate state.

We will include more details of this validation in the revised manuscript. Our method gave results in reasonable agreement with the climate model at equilibrium: "We analyzed runs of the fully coupled Max Planck Institute Earth System Model version 1.1 (MPI-ESM1.1) (Maher et al., 2019), which has a transient climate response and an effective climate sensitivity near the

middle of the CMIP5 ensemble range (Adams and Dessler, 2019; Dessler, 2020). It includes a 2000-year preindustrial control run and a 2614-year abruptly quadrupled CO_2 run. The values of ΔSWV averaged over the last 30 years of the $4xCO_2$ run relative to the control run are 4.60 ppmv in the TLS, 22.40 ppmv in the NH LMS, and 9.69 ppmv in the SH LMS. We expect this to be close to equilibrium ΔSWV because the trend in global average surface temperature over the last 500 years of the $4xCO_2$ run is 0.02 K per century. We use the regression method to estimate the equilibrium ΔSWV using MPI-ESM1.1 water vapor mixing ratio time series over the first 100 years and obtain estimates of 4.38 ppmv in the TLS, 20.01 ppmv in the NH LMS, and 9.07 ppmv in the SH LMS; these yield differences of 0.22 ppmv in the TLS, 2.39 ppmv in the NH LMS, and 0.62 ppmv in the SH LMS. Thus, our method underestimates the true equilibrium value by 5% in the TLS, 11% in the NH LMS, and 6% in the SH LMS."

We will also produce estimates using the last 30 years, and we will add those to a table in the supplementary material.

"3. It may be worth pointing out how the PDRMIP model ensembles relate to the CMIP5 ensembles. From Fig. 2b, it seems that all of these models except HadGEM3 are on the weaker side of the CMIP5 ECS estimation range. I am also surprised to see that these models do not show an more distinct efficacy among different forcing agents (Hansen et al. 2005)."

The PDRMIP models are a subset of the CMIP5 models. The PDRMIP multi-model average ECS we estimated is 3.6 K, which is 10% larger than the whole CMIP5 ensemble (3.3 K) (Zelinka et al. 2020). We will add a statement to the revised manuscript comparing the PDRMIP models' ECS to that in the CMIP5 ensemble.

As far as forcing efficacy goes, Hansenet al. (2005) also pointed out that efficacies depend on the method of which radiative forcing is defined. A more recent paper by Richardson et al. (2019) (which we already referenced in the submitted manuscript) using PDRMIP data showed that forcing efficacies calculated from effective radiative forcing have values close to one. Our results are in good agreement with that paper.

"4. The authors relate the slow response to the surface temperature and relate the fast response to the cold point temperature. I believe the slow response would also be regulated by the cold point temperature. It may be interesting to show that if the relationship between the stratospheric water vapor and the cold point temperature holds from the fast adjustment to the slow response."

It certainly may be the case that the slow response is mediated by TTL temperatures, but by no means is that certain. Dessler et al. (2016) showed that, in two climate models, at least, a significant fraction of the long-term trend (and slow response) was due to increases in convective moistening, which bypasses the TTL cool trap.

We have done analyses testing whether the PDRMIP models and experiments show agreement for the relation between ΔSWV_{slow} vs the CPT slow response (Figure R3). Results from the models and experiments show good agreement. The slope is 0.72 ppmv/K, which is larger than the slope obtained from the fast response. Nevertheless, correlation does not prove causality and this result could arise from either TTL control or if convective moistening also correlates with the CPT slow response, or some combination. We will add a sentence to the paper describing this analysis.

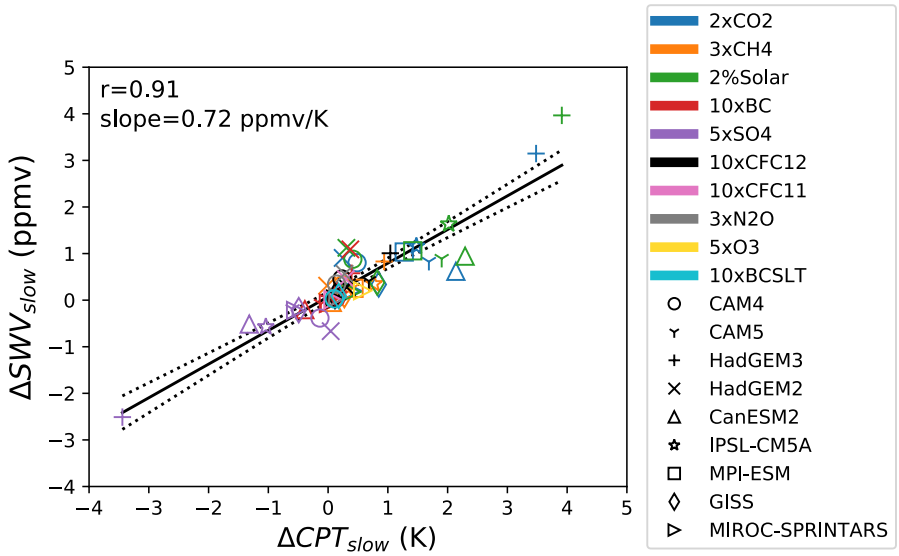

Figure R3: Same as Figure 6a of the submitted manuscript, but for TLS SWV slow response vs the CPT slow response.

"5. While Fig. 3 shows a consistent relationship between stratospheric water vapor and global mean surface temperature across various forcing, the temperature sensitivity does not seem to be so consistent in Fig. S4. Much more stratospheric moistening is seen in response to the solar forcing than others given the same surface temperature warming. This discrepancy needs to be resolved."

We list the regression slope values in Table R4 below. These values are the same as we have shown in Fig. 3 of the submitted manuscript. It may not be clear in Fig. 3 of the submitted manuscript, but it is clear in Table R4 below that the sensitivities are indeed larger in some experiments, such as the 2%Solar experiment. This is the same for slopes computed using the two different units – ppmv/K and %/K (listed in the parentheses).

We will add Table R4 to the supplement of the revised manuscript.

Table R4: Regression slope of ΔSWV_{slow} annual mean time series vs surface temperature change annual mean time series for all perturbations and models. The unit of the values is ppmv/K. The unit of the values in parentheses is %/K.

TLS SWV

	2xCO2	3xCH4	2%SOLAR	10xBC	5xSO4	10xCFC12	10xCFC11	3xN2O	5xO3	10xBCTAU
CAM4	0.26 (6.35)	0.25 (6.19)	0.30 (7.27)	0.34 (8.44)	0.31 (7.64)	0.27 (6.50)	nan	0.29 (7.04)	nan	0.18 (4.44)
CAM5	0.36 (9.74)	0.26 (6.98)	0.36 (9.76)	0.11 (3.05)	0.11 (3.06)	0.23 (6.23)	nan	nan	nan	nan
HadGEM3	0.92 (17.89)	0.64 (12.47)	1.01 (19.64)	0.54 (10.48)	0.40 (7.86)	0.70 (13.56)	nan	nan	nan	nan
HadGEM2	0.46 (9.22)	0.43 (8.52)	0.60 (11.94)	1.78 (35.29)	0.35 (6.95)	0.63 (12.49)	0.67 (13.34)	0.66 (13.05)	nan	nan
CanESM2	0.27 (10.25)	-0.01 (-0.23)	0.38 (14.59)	0.12 (4.68)	0.12 (4.77)	nan	nan	nan	nan	nan
IPSL-CM5A	0.62 (26.79)	0.36 (15.52)	0.79 (33.70)	0.52 (22.30)	0.28 (11.78)	nan	nan	nan	nan	nan
MPI-ESM	0.53 (12.78)	0.22 (5.22)	0.54 (12.95)	nan	nan	nan	nan	nan	nan	nan
GISS	0.28 (16.28)	0.16 (9.05)	0.31 (18.17)	0.25 (14.80)	0.20 (11.73)	0.18 (10.23)	nan	nan	nan	0.15 (8.53)
MIROC-SPRINTARS	0.08 (2.61)	0.11 (4.07)	0.14 (5.04)	0.09 (3.15)	0.09 (3.26)	0.14 (5.06)	0.10 (3.64)	0.08 (2.83)	0.05 (1.59)	nan
ensemble average	0.42 (12.43)	0.27 (7.53)	0.49 (14.78)	0.47 (12.77)	0.23 (7.13)	0.36 (9.01)	0.39 (8.49)	0.34 (7.64)	0.05 (1.59)	0.16 (6.49)

NH LMS SWV

	2xCO2	3xCH4	2%SOLAR	10xBC	5xSO4	10xCFC12	10xCFC11	3xN2O	5xO3	10xBCTAU
CAM4	2.67 (11.63)	1.55 (6.71)	2.47 (10.75)	2.41 (10.49)	1.91 (8.50)	2.08 (8.84)	nan	1.22 (5.18)	nan	0.58 (2.44)
CAM5	1.67 (7.70)	-0.26 (-0.59)	1.77 (8.28)	-0.35 (-0.75)	0.90 (4.35)	0.30 (1.85)	nan	nan	nan	nan
HadGEM3	4.31 (27.80)	3.19 (20.72)	5.15 (33.01)	3.84 (24.77)	1.60 (10.22)	3.49 (22.56)	nan	nan	nan	nan
HadGEM2	2.17 (20.79)	1.71 (16.08)	2.44 (23.34)	3.99 (38.14)	1.20 (11.47)	2.08 (19.87)	2.03 (19.42)	2.02 (19.33)	nan	nan
CanESM2	3.18 (22.65)	2.61 (18.76)	3.37 (23.85)	3.59 (25.94)	2.00 (14.31)	nan	nan	nan	nan	nan
IPSL-CM5A	2.42 (16.09)	1.94 (13.21)	2.81 (18.59)	2.38 (15.88)	1.94 (13.05)	nan	nan	nan	nan	nan
MPI-ESM	2.56 (12.29)	1.56 (7.45)	2.36 (11.26)	nan	nan	nan	nan	nan	nan	nan
GISS	1.19 (15.55)	0.72 (8.90)	1.12 (14.45)	1.05 (13.67)	0.73 (8.84)	0.76 (9.06)	nan	nan	nan	0.93 (11.54)
MIROC-SPRINTARS	2.45 (19.18)	2.30 (19.20)	2.40 (18.69)	2.81 (22.27)	1.85 (14.13)	3.00 (23.59)	2.42 (19.15)	2.20 (17.99)	3.36 (24.67)	nan
ensemble average	2.52 (17.08)	1.70 (12.27)	2.65 (18.02)	2.46 (18.80)	1.52 (10.61)	1.95 (14.29)	2.23 (19.29)	1.82 (14.17)	3.36 (24.67)	0.76 (6.99)

SH LMS SWV

SH LMS SWV	2xCO2	3xCH4	2%SOLAR	10xBC	5xSO4	10xCFC12	10xCFC11	3xN2O	5xO3	10xBCTAU
CAM4	1.67 (11.05)	1.53 (10.87)	1.88 (12.55)	0.61 (4.70)	0.84 (5.44)	1.76 (11.75)	nan	1.21 (8.44)	nan	0.84 (6.39)
CAM5	0.87 (5.60)	-0.14 (0.47)	0.99 (6.22)	-0.53 (-2.24)	0.34 (2.68)	-0.38 (-1.03)	nan	nan	nan	nan
HadGEM3	2.65 (22.08)	1.63 (14.66)	3.05 (25.21)	0.90 (8.17)	1.15 (9.91)	1.75 (14.81)	nan	nan	nan	nan
HadGEM2	0.93 (12.88)	0.61 (8.59)	0.94 (13.33)	1.08 (15.47)	0.58 (8.10)	0.63 (9.15)	0.60 (8.67)	0.78 (10.96)	nan	nan
CanESM2	1.24 (12.11)	0.64 (6.68)	1.36 (13.02)	1.50 (14.70)	0.85 (8.19)	nan	nan	nan	nan	nan
IPSL-CM5A	1.60 (15.84)	1.08 (11.08)	1.74 (16.82)	0.63 (6.53)	1.11 (11.64)	nan	nan	nan	nan	nan
MPI-ESM	1.34 (9.87)	0.80 (6.12)	1.45 (10.76)	nan	nan	nan	nan	nan	nan	nan
GISS	0.65 (11.44)	-0.09 (-0.27)	0.80 (14.48)	0.00 (1.15)	0.21 (4.54)	0.01 (1.61)	nan	nan	nan	0.32 (5.85)
MIROC-SPRINTARS	1.16 (10.88)	0.82 (7.72)	1.14 (10.63)	0.80 (8.10)	0.88 (7.93)	1.29 (11.97)	0.78 (7.49)	0.80 (7.81)	1.34 (12.30)	nan
ensemble average	1.35 (12.42)	0.76 (7.33)	1.48 (13.67)	0.62 (7.07)	0.75 (7.31)	0.84 (8.04)	0.69 (8.08)	0.93 (9.07)	1.34 (12.30)	0.58 (6.12)

"Line 85-86: How does the averaged of fixed SST with baseline atmosphere compare to the average of the coupled baseline simulations."

For TLS SWV, the difference between fixed SST baseline simulation and coupled baseline simulation is on the order of 0.01 – 1 ppmv. For LMS SWV, the difference between fixed SST baseline simulation and coupled baseline simulation is on the order of 0.1 – 1 ppmv.

The results are averaged over the entire period of the baseline simulations for both fixed SST run and coupled run.

"Line 96: y=c+abˆx -> y=c+abˆ(-x)

Line 101: Fig. S1 was not showing what is stated here. It seems the intended Fig. S1 is missing.

Line 147: Fig. S2-4. -> Fig. S1-3

Line 167: Fig. S5 -> Fig. S4"

We have updated these in the manuscript.

"Line 191: Does the long wave effect of the tropospheric ozone also contribute?"

Yes, the tropospheric ozone has the long wave radiative effect. We are going to edit the text to "Increases of tropospheric O_3 ($5xO_3$) reduce the upwelling longwave radiation through longwave absorption, which cools the stratosphere…"

References

Adams, B. K. and Dessler, A. E.: Estimating Transient Climate Response in a Large-Ensemble Global Climate Model Simulation, Geophys. Res. Lett., 46(1), 311–317, doi:10.1029/2018GL080714, 2019.

Banerjee, A., Chiodo, G., Previdi, M., Ponater, M., Conley, A. J. and Polvani, L. M.: Stratospheric water vapor: an important climate feedback, Clim. Dyn., doi:10.1007/s00382-019-04721-4, 2019.

Dessler, A. E.: Potential Problems Measuring Climate Sensitivity from the Historical Record, J. Clim., 33(6), 2237–2248, doi:10.1175/JCLI-D-19-0476.1, 2020.

Dessler, A. E., Schoeberl, M. R., Wang, T., Davis, S. M. and Rosenlof, K. H.: Stratospheric water vapor feedback, Proc. Natl. Acad. Sci., 110(45), 18087–18091, doi:10.1073/pnas.1310344110, 2013.

Dessler, A. E., Ye, H., Wang, T., Schoeberl, M. R., Oman, L. D., Douglass, A. R., Butler, A. H., Rosenlof, K. H., Davis, S. M. and Portmann, R. W.: Transport of ice into the stratosphere and the humidification of the stratosphere over the 21st century, Geophys. Res. Lett., 43(5), 2323–2329, doi:10.1002/2016GL067991, 2016.

Fueglistaler, S.: Stratospheric water vapor predicted from the Lagrangian temperature history of air entering the stratosphere in the tropics, J. Geophys. Res., 110(D8), D08107, doi:10.1029/2004JD005516, 2005.

Fueglistaler, S., Dessler, A. E., Dunkerton, T. J., Folkins, I., Fu, Q. and Mote, P. W.: Tropical tropopause layer, Rev. Geophys., 47, 1–31, doi:10.1029/2008RG000267, 2009.

Hansen, J.: Efficacy of climate forcings, J. Geophys. Res., 110(D18), D18104, doi:10.1029/2005JD005776, 2005.

Maher, N., Milinski, S., Suarez-Gutierrez, L., Botzet, M., Dobrynin, M., Kornblueh, L., Kröger, J., Takano, Y., Ghosh, R., Hedemann, C., Li, C., Li, H., Manzini, E., Notz, D., Putrasahan, D., Boysen, L., Claussen, M., Ilyina, T., Olonscheck, D., Raddatz, T., Stevens, B. and Marotzke, J.: The Max Planck Institute Grand Ensemble: Enabling the Exploration of Climate System Variability, J. Adv. Model. Earth Syst., 11(7), 2050–2069, doi:10.1029/2019MS001639, 2019.

Mote, P. W., Rosenlof, K. H., McIntyre, M. E., Carr, E. S., Gille, J. C., Holton, J. R., Kinnersley, J. S., Pumphrey, H. C., Russell III, J. M. and Waters, J. W.: An atmospheric tape recorder: The imprint of tropical tropopause temperatures on stratospheric water vapor, J. Geophys. Res., 101(D2), 3989–4006, doi:10.1029/95JD03422, 1996.

Richardson, T. B., Forster, P. M., Smith, C. J., Maycock, A. C., Wood, T., Andrews, T., Boucher, O., Faluvegi, G., Fläschner, D., Hodnebrog, Ø., Kasoar, M., Kirkevåg, A., Lamarque, J. -F., Mülmenstädt, J., Myhre, G., Olivié, D., Portmann, R. W., Samset, B. H., Shawki, D., Shindell, D., Stier, P., Takemura, T., Voulgarakis, A. and Watson-Parris, D.: Efficacy of Climate Forcings in PDRMIP Models, J. Geophys. Res. Atmos., 124(23), 12824–12844, doi:10.1029/2019JD030581, 2019.

Zelinka, M. D., T. A. Myers, D. T. McCoy, S. Po-Chedley, P. M. Caldwell, P. Ceppi, S. A. Klein, and K. E. Taylor, 2020: Causes of higher climate sensitivity in CMIP6 models, Geophys. Res. Lett., 47, doi:10.1029/2019GL085782.